Native CRISPR-Cas mediated in situ genome editing reveals the exquisite interplay of resistance mutations in clinical multidrug resistant *Pseudomonas aeruginosa*

Zeling Xu, [1¶] Ming Li,[2¶] Yanran Li,[1] Huiluo Cao,[1,#] Patrick CY Woo,[3] Hua Xiang,[2*] Aixin Yan[1*]

[1] School of Biological Sciences, The University of Hong Kong, Hong Kong SAR, China

[2] State Key Laboratory of Microbial Resources, Institute of Microbiology, Chinese Academy of Sciences, Beijing, China

[3] Department of Microbiology, Li Ka Shing Faculty of Medicine, The University of Hong Kong, Hong Kong SAR, China

[#] Current Address: Department of Microbiology, Li Ka Shing Faculty of Medicine, The University of Hong Kong, Hong Kong SAR, China

* Corresponding author

E-mail: xiangh@im.ac.cn (HX) or ayan8@hku.hk (AY)

[¶] These authors contributed equally to this work.

Short title: Harnessing the native CRISPR-Cas system to tackle clinical multidrug resistance

Abstract

Antimicrobial resistance (AMR) is imposing a global public health threat. Despite its importance, resistance characterization in the native background of clinically isolated resistant pathogens is frequently hindered by the lack of genome editing tools in these "non-model" strains. *Pseudomonas aeruginosa* is both a prototypical multidrug resistant (MDR) pathogen and a model species for understanding CRISPR-Cas functions. In this study, we report the successful development of the first native type I-F CRISPR-Cas mediated, one-step genome editing technique in a paradigmatic MDR strain PA154197. The technique is readily applicable in additional type I-F CRISPR-containing, clinical/environmental *P. aeruginosa* isolates. A two-step In-Del strategy is further developed to edit genomic locus lacking an effective PAM (protospacer adjacent motif) or within an essential gene, which together principally allows any type of non-lethal genomic manipulations in these strains. Exploiting these powerful techniques, a series of reverse mutations are constructed and the key resistant determinants of the MDR PA154197 are elucidated which include over-production of two multidrug efflux pumps MexAB-OprM and MexEF-OprN, and a typical fluoroquinolone (FQ) resistance mutation T83I in the drug target gene *gyrA*. Characterizing antimicrobial susceptibilities in isogenic strains containing various combinations of single, double, or all three key resistance determinants reveal that i) extensive synergy exists between the target mutation and over-production of efflux pumps, and between the two over-produced tripartite efflux pumps to confer clinically significant FQ resistance; ii) while basal level MexAB-OprM confers resistance only to penicillins, its over-production leads to substantial resistance to all antipseudonmonal β-lactams and additional resistance to FQs; iii) despite the acquisition and over-production of multiple resistant mutations, no obvious evolutionary trade-off of collateral sensitivity is developed in PA154197. Together, these results provide new insights into

47 resistance development in clinical MDR *P. aeruginosa* strains and demonstrate the great
48 potentials of native CRISPR systems in AMR research.

49

50 Author Summary

51 Genome editing and manipulation can revolutionize the understanding, exploitation, and
52 control of microbial species. Despite the presence of well-established genetic manipulation
53 tools in various model strains, their applicability in the medically, environmentally, and
54 industrially important, "non-model" strains is often hampered owing to the vast diversity of
55 DNA homeostasis in these strains and the cytotoxicity of the heterologous CRISPR-Cas9/Cpf1
56 systems. Harnessing the native CRISPR-Cas systems broadly distributed in prokaryotes with
57 built-in genome targeting activity presents a promising and effective approach to resolve these
58 obstacles. We explored and exploited this methodology in the prototypical multidrug resistant
59 (MDR) pathogen *P. aeruginosa* by exploiting the most common subtype of the native CRISPR
60 systems in the species. Our successful development of the first type I-F CRISPR-mediated
61 genome editing technique and its subsequent extension to additional clinical and environmental
62 *P. aeruginosa* isolates opens a new avenue to the functional genomics of antimicrobial
63 resistance. As a proof-of-concept, we characterized the resistance development in a
64 paradigmatic MDR *P. aeruginosa* isolate and found extensive resistance synergy and the lack
65 of collateral sensitivity in the strain, implying the extraordinary pathoadaptation capability of
66 clinical MDR strains and challenges to eradicate them.

67

68 Introduction

Antimicrobial resistance (AMR) is imposing an alarming threat to the global public health. Of particular challenging in clinics are those "ESKAPE" pathogens which constitute the major sources of nosocomial infections and are extraordinary to engender resistance, i.e. *Enterococcus spp.*, *Staphylococcus aureus*, *Klebsiella spp.*, *Acinetobacter baumannii*, *Pseudomonas aeruginosa*, and *Enterobacter spp.*. Owing to its intrinsic resistance to a variety of antimicrobials and the enormous capacity of developing acquired resistance during antibiotics chemotherapies, *Pseudomonas aeruginosa* is recognized as the prototypical multidrug resistant (MDR) pathogen [1-4]. Remarkably, in recent years, international high-risk clones of MDR *P. aeruginosa* have emerged and have been shown to cause worldwide outbreaks [5]. Genetic analyses reveal that these clones often contain a complex set of resistance markers [6-8] including both the genetic variations that cause resistance to specific classes of antibiotics, such as mutations in drug targets and acquisition of drug modification enzymes, and those conferring simultaneous resistance to multiple drugs, such as over-expression of multidrug efflux pumps. However, key genetic mutations responsible for the MDR development of clinically significant resistant isolates in their native genetic backgrounds remain undetermined. Furthermore, relative contributions and the interplay of different resistance determinants which shape the MDR profile of resistant isolates and imply the corresponding treatment regimens remain largely elusive.

Current knowledge of the resistance determinants and their mechanisms are largely obtained by reconstitution in laboratory model strains [9, 10]. Several studies indicated that there is a lack of multiplicative or synergetic effects between over-expression of multidrug efflux pumps, and between efflux and the mechanisms causing resistance to specific classes of antibiotics, such as over-expression of the cephalosporinase AmpC and mutations in the DNA gyrase GyrA or topoisomerase IV ParC [11-14]. It was reported that synergistic interactions occur when different types of multidrug efflux systems operate simultaneously, i.e. the tripartite resistance-

nodulation-division (RND) efflux pumps and the single component pump (e.g. TetA/C) [15]. Antagonistic interplay of different RND efflux pumps was also reported, especially in the *nfxC* type MDR *P. aeruginosa* isolates in which over-production of the MexEF-OprN pump is often concomitant with an impairment of the MexAB-OprM pump in the strain, resulting in a high resistance to quinolones but a hyper-susceptibility to β-lactams [16, 17]. Compounding the complexity of the resistant mutation networks is the effect of genetic background of resistant strains and epistasis among different resistant mutations which are increasingly recognized to play important roles in resistance development and affect the effectiveness of antibiotic chemotherapies [18-20]. Hence, it is necessary to identify the key resistant determinants and their collateral effects in the native genetic background of clinical MDR strains. Yet, these molecular characterizations are often hindered by the lack of efficient and readily applicable genomic editing tools in these "non-model" strains.

In addition to be a prototypical MDR pathogen, *P. aeruginosa* is an important model system for understating CRISPR-Cas functions, especially the type I CRISPR-Cas system. Phylogenetic analysis revealed that CRISPR-Cas systems are widely distributed in global AMR *P. aeruginosa* isolates with more than 90% belonging to the I-E or I-F subtypes [21]. Owing to its built-in genome targeting activity and reprogrammable feature, in recent years, repurposing the native CRISPR-Cas systems present in the large number of prokaryotes for genetic editing is emerging as a promising strategy for functional genetics, especially in those species with low transformation efficiency and poor homologous recombination. For instance, the native type I-B CRISPR-Cas system in *C. tyrobutyricum*, *C. pasteurianum*, *H. hispanica* (archaea) and the type I-A & III-B native CRISPR-Cas systems in *S. islandicus* (archaea) have been successfully harnessed for genome editing in the corresponding species recently [22-25]. Whether the broadly distributed native CRISPR-Cas systems in *P. aeruginosa*, especially the

most common subtype of I-F, can be harnessed for genome editing and functional genomics of antimicrobial resistance remains unexplored.

Previously, we have isolated a MDR *P. aeruginosa* strain PA154197 which displays high epidemic potentials with a resistance profile (resistant to five of the seven commonly used antipseudomonal drugs) comparable to the international high-risk clone ST175 [26]. A large number of resistant mutations were predicted by genomic analysis, including mutations in the DNA gyrase *gyrA* and Cephalosporinase *ampC* which are associated with resistance to fluoroquinolones (FQ) and β-lactams [27, 28], respectively, and gene mutations potentially causing over-production of three multidrug efflux pumps MexAB, MexEF, and MexGHI (S1 Table). Genome sequencing reveals that PA154197 contains a native type I-F CRISPR-Cas locus. These together renders PA154197 a paradigm to explore the harnessing of a native type I-F CRISPR-Cas system for genome editing in a clinical MDR *P. aeruginosa* strain and exploiting the system for AMR characterization in its native genetic background.

In this study, we report the successful development of a single plasmid-mediated, one-step, precise genomic manipulation technique in PA154197 by exploiting its native type I-F CRISPR-Cas system, and a two-step In-Del approach to edit the genomic loci lacking an effective PAM (protospacer adjacent motif) sequence. Exploiting this efficient and powerful technique, a series of single, double, and triple mutations of key resistant determinants are constructed, and their interplay in resistance synergy and potential collateral effects are investigated, providing a comprehensive functional genetics investigation of clinical MDR which have implications in clinical treatment of MDR infections. Lastly, we examine the applicability of the established editing technique in two additional type I-F CRISPR-containing, clinical and environmental *P. aeruginosa* strains PA150567 and Ocean-100. Together, these results demonstrate the general applicability of native CRISPR-based editing system in the

142 characterization of resistance development of clinical MDR *P. aeruginosa* isolates, and
143 presumably other species.
144

145 ## Results

146 **PA154197 contains a functional type I-F CRISPR-Cas system.**

147 Analysing the genome sequence of PA154197 reveals the presence of the signature *cas8f* and
148 *cas6f* genes and the unique *cas2-cas3* fusion in its CRISPR-Cas loci, suggesting that the system
149 belongs to the subtype I-F (Fig 1A) [29]. The *cas* operon of the system is found to be
150 sandwiched by two convergent CRISPRs. Their consensus repeat sequence differs by only one
151 nucleotide, and their spacers are nearly identical in size (32 bp). In addition, a number of
152 spacers show significant homology to phage or putative prophage sequences (data not shown),
153 suggesting the DNA interference potential of this CRISPR-Cas system and the feasibility of
154 exploiting the system for genome editing.
155 To harness the native CRISPR-Cas for genome editing, it is necessary to first examine its
156 endogenous genome targeting activity. We select *mexB* as the target gene for this purpose,
157 which encodes the inner membrane component of the housekeeping efflux system MexAB-
158 OprM. Previous studies revealed that the canonical target of the type I-F CRISPR-Cas system
159 is 5'-CC-protospacer-3' [30] (note that our study follows the standard guide-centric PAM
160 definition [31]). Hence, an internal 32-bp sequence preceded by a 5'-CC-3' PAM in *mexB* is
161 selected as the target (PAM-protospacer). A functional mini-CRISPR which is composed of
162 the 32-bp spacer flanked by 28-bp repeat sequences at both ends is then synthesized and cloned
163 into the expression vector pMS402, which contains a kanamycin-resistant gene and a *lux*
164 reporter cassette [32], to generate the targeting plasmid pAY5233 (Fig 1B). To ensure the
165 expression of the mini-CRISPR and efficient targeting, a strong promoter P*tat* [33] is selected

and cloned upstream to drive its expression in pAY5233. To overcome the poor antibiotics-based selection of transformants in MDR strains, the P*tat*-mini-CRISPR is positioned upstream of the *lux* operon in frame in pAY5233 such that P*tat* simultaneously drives the expression of both the CRISPR element and the *lux* operon which assists the transformant screening (Fig 1B). When the targeting plasmid pAY5233 and the control plasmid pAY5211 (which contains all the elements described above except the mini-CRISPR fragment) were introduced into PA154197 cells, a dramatic decrease of the transformants recovery was observed comparing to the non-targeting control (Fig 1C), implying the occurrence of the detrimental chromosome cleavage in the pAY5233-containing cells. This result confirms that the native CRISPR-Cas system is active in PA154197.

Harnessing the native type I-F CRISPR-Cas system to delete the resistance gene *mexB*.

To exploit the system for gene deletion (Δ*mexB* as an example), we then assemble a 1-kb donor sequence consisting of the 500-bp upstream and 500-bp downstream of *mexB* for homologous recombination, and insert it into pAY5233 to yield pAY5235, termed as the editing plasmid (Fig 1D). The number of transformants of pAY5235 is significantly increased (by more than 10-fold) compared to pAY5233 (Fig 1C), suggesting the occurrence of homologous recombination by provision of the donor sequence. We randomly selected eight luminescence positive colonies for validation and found four colonies showed the desired, scarless and precise deletion of *mexB* in the chromosome (Fig 1E and 1F). These results demonstrate the success of genome editing by exploitation of the native type I-F CRISPR-Cas system in the clinical MDR isolate PA154197 by one-step introduction of a single editing plasmid.

The success rate of 4/8 seemed moderate. However, we speculate that it was due to the unusually large size (3141 bp) of *mexB* rather than the efficiency of the editing technique, as subsequent attempts to delete shorter fragments, i.e. 50-bp, 500-bp, or 1000-bp within *mexB*

(S1A Fig), yielded significantly improved success rate, i.e. 8/8 (50-bp deletion), 7/8 (500-bp deletion), and 7/8 (1000-bp deletion) (S1B Fig). Given that the average length of a prokaryotic gene is ~1 kb [34], the native CRISPR-based editing strategy we developed is efficient to knock out a target gene. Indeed, the 4/8 successful rate for the 3-kb *mexB* is fairly high according to several recent reports [35, 36]. Moreover, we found the editing plasmid can be readily cured following culturing the edited cells in the absence of the antibiotic (kanamycin) pressure overnight (S2 Fig), suggesting the feasibility of multiple rounds of gene editing using the reprogrammable pAY5235 editing platform.

To examine the applicability of the technique in other type I-F CRISPR-Cas containing *P. aeruginosa* strains, we set out to construct *mexB* deletion in a carbapenem resistant clinical strain PA150567 (accession number: LSQQ00000000) isolated from the Queen Mary Hospital, Hong Kong and an environmental strain Ocean-100 (accession number: NMRS00000000) isolated from the North Pacific Ocean [37]. As expected, transformation of the targeting plasmid pAY5233 led to DNA interference in the two strains, and the editing plasmid pAY5235 achieved the desired *mexB* deletion with comparable successful rate as in PA154197 (S3 Fig), confirming the general applicability of the developed editing system in clinically and environmentally isolated, "non-model" *P. aeruginosa* strains.

Over-expression of the MexAB-OprM and MexEF-OprN efflux pumps contributes substantially to the MDR of PA154197.

Three multidrug efflux pumps MexAB-OprM, MexEF-OprN, MexGHI-OpmD were found to be hyper-expressed in PA154197 compared to PAO1 [26]. To test their contribution to the MDR phenotype of the strain, we first delete *mexB*, *mexF*, and *mexH*, which encodes the inner membrane channel of the three efflux systems, respectively. We find that except for IPM, Δ*mexB* leads to substantial decrease in the MICs of all antipseudomonal antibiotics PA154197

is resistant to (Fig 2 and S2 Table), i.e. ATM (64 fold), CAZ (8 fold), TZP (64 fold), MEM (> 32 fold), CAR (>128 fold), LVX (2 fold), and CIP (2 fold), with a greater effect on the antipseudomonal β-lactams (CAR, CAZ, MEM, ATM), and penicillin-β-lactamase inhibitor combinations (TZP) than on fluoroquinolones (LVX and CIP). Δ*mexF* leads to the decrease in MICs of antipseudomonal fluoroquinolones, i.e. LVX (2 fold) and CIP (4 fold), consistent with the previous report of their substrates profiles by ectopic over-expression of the pumps in PAO1 [38]. Double deletion of *mexB* and *mexF* leads to dramatic decrease in MICs of all antipseudomonal antibiotics (except IPM) and several other antimicrobial agents tested (Fig 2 and S2 Table), suggesting that hyper-active drug efflux by these two pumps contributes substantially to the MDR profile of PA154197. Moreover, different from the observations obtained by over-expressing the pumps in *E. coli* which showed no synergy between two tripartite pumps [15], substantial synergy is observed between the over-expressed MexAB-OprM and MexEF-OprN pumps in PA154197 to expel their common substrates FQs as evidenced by the MIC values in the Δ*mexB* Δ*mexF* double deletion strain relative to that in Δ*mexB* and Δ*mexF* single deletion strain. Quantifying these interaction using the fractional inhibitory concentration index (FICI) [39] also demonstrates the substantial synergy of the two pumps in LVX (FICI 0.125) and CIP (FICI 0.188) resistance (Fig 2). Disk diffusion test confirms the susceptibility changes in these strains (S4 Fig). Analysis of the growth curves of these strains in the absence of antibiotics suggests that the observed MIC alterations are not due to intrinsic disadvantages or defects in growth (S5 Fig). Unexpectedly, deletion of another efflux gene *mexH* which is also hyper-expressed in PA154197 (~40-fold higher than in PAO1) [26] does not lead to any detectable difference in the MICs of all the antibiotics and antimicrobial agents tested (Fig 2 and S2 Table). Further deletion of *mexH* in the Δ*mexB* Δ*mexF* strain yields no MIC change either (data not shown), suggesting that it does not contribute to the antibiotic resistance in PA154197.

A G226T point mutation in *mexR* is responsible for the *mexAB-oprM* over-expression.

Over-expression of efflux genes is often caused by mutations in their transcription regulators. Comparative genomic analysis revealed a single nucleotide substitution G226T (corresponding to introducing a stop codon following E76) in PA154197 *mexR* compared to PAO1 (S6A Fig). Mutations or pre-mature termination of the MexR often leads to over-production of the MexAB-OprM pump (Fig 3A) and MDR in the cells [40-42]. To investigate whether this point mutation accounts for the over-expression of *mexAB-oprM* in PA154197, we reprogramed the editing plasmid pAY5235 by replacing the mini-CRISPR and the donor sequences for deleting *mexB* with those for point mutation of *mexR*, respectively, and constructed the reverse mutation T226G. The resulting construct is designated as $mexR^{PAO1}$. Transcriptional level of *mexAB* genes in the $mexR^{PAO1}$ mutant is found to be significantly reduced comparing with that in the wild-type (WT) PA154197, to a level that is similar in PAO1 (Fig 3B), suggesting that the G226T mutation in *mexR* is responsible for the over-expression of *mexAB-oprM*. Both MIC analysis and disk diffusion test confirm that $mexR^{PAO1}$ causes decreases in MICs of all MexAB-OprM substrates (Fig 2 and S4 Fig).

An advanced two-step In-Del strategy to edit *mexT* verifies its role in *mexEF-oprN* over-expression and reduced *oprD* expression.

The *mexT* gene encodes a transcription regulator of the *mexEF-oprN* efflux system (Fig 3A) [9]. Comparative genomic analysis identified an 8-bp deletion in PA154197 *mexT* (S6B Fig), a *nfxC* type resistant mutation which is proposed to convert the intrinsically inactive, out-of-frame variant of *mexT* as that encoded in PAO1 to a translationally in-framed active MexT that activates *mexEF-oprN* [43, 44]. To verify this effect in the MDR strain PA154197, we attempted to construct the 8-bp insertion reverse mutation. However, construction using the

same one-step strategy for gene deletion and point mutation described above was not successful (S7 Fig). Analysing the nucleotides sequence of the PAM-protospacer for the 8-bp insertion reveals the presence of two 6-bp repeats, which potentially obscures the CRISPR recognition of the PAM and the subsequent DNA interference (S7 Fig).

To overcome this limitation, we devise a two-step Insert-Delete (In-Del) strategy to edit this inefficiently targeted site (Fig 4A). The approach bypasses the poorly targeted PAM-protospacer by exploiting a proximal, auxiliary PAM (152-bp downstream of the desired 8-bp insertion site) which can be efficiently targeted to firstly insert a 32-bp short tag (5'-TACAACAAGGACGACGACGACAAGGTGATCAG-3') between the PAM and the protospacer. The editing of introducing a short tag is applied as both its insertion and subsequent removal is highly efficient. The desired 8-bp insertion is then achieved in the second round of editing during which the short tag is deleted by exploiting the same PAM as in the first step but a different protospacer sequence (termed as the PAM-tag-protospacer) and the provision of a donor sequence which lacks the tag but contains the desired insertion sequence (Fig 4A). The success rate for the first and second round editing for 8-bp insertion in *mexT* is found to be 8/8 and 5/8 (Fig 4B and 4C). This In-Del strategy presumably allows any type of non-lethal genetic manipulations regardless of PAM limitation.

The resulting mutant is designated as $mexT^{PAO1}$. As expected, both transcription of *mexEF* and the MICs of LVX and CIP in the $mexT^{PAO1}$ cells is reduced comparing with the WT PA154197 (Fig 3C, Fig 2, S2 Table), confirming that the *nfxC* type mutation (8-bp deletion in *mexT*) is responsible for the over-expression of *mexEF-oprN* and contributes to FQ resistance in PA154197. Consistent with the previous report of the *nfxC* type resistant mutation, the reverse mutation $mexT^{PAO1}$ also leads to a 3-fold higher transcription of *oprD* than the PA154197 parent (Fig 3C), which encodes a porin protein facilitating the diffusion of carbapenems antibiotics (especially IPM), and an increased susceptibility to IPM in PA154197 (Fig 2 and S4 Fig).

Together, these results indicate that PA154197 may derive from a *nfxC* type resistant strain with acquired resistance to fluoroquinolones and tolerance to IPM (breaking point of IPM is 4). A two-component system ParSR is also known to be involved in regulating *mexEF-oprN* [45]. A nonsynonymous nucleotide substitution G1193A is identified in PA154197 *parS* (S1 Table), However, reverse mutation in this gene does not reveal any susceptibility changes (S2 Table), suggesting this mutation does not contribute to the antibiotic resistance development in PA154197.

Mutations in the essential gene *gyrA* constitute the third fluoroquinolone resistance determinant in PA154197.

Although Δ*mexB* Δ*mexF* leads to a dramatic decrease (32 fold) in MICs of the fluoroquinolones LVX (32 to 1) and CIP (16 to 0.5), the strain still displays a lower susceptibility to these two antibiotics than PAO1 (MIC of both LVX and CIP are 0.25), suggesting the presence of additional FQ resistance determinants in PA154197. A well-studied T248C substitution (corresponding to T83I) in the quinolone resistance determining region (QRDR) which abolishes (fluoro)quinolone binding [46] is identified in the PA154197 DNA gyrase gene *gyrA* (S6C Fig). To verify its role in the high FQ resistance of PA154197 and interaction with the other two FQ resistance determinants identified, we employ the two-step In-Del strategy described for the 8-bp insertion in *mexT* to replace the essential gene *gyrA* in PA154197 with that from PAO1, generating $gyrA^{PAO1}$ (S8 Fig). It is found that this gene replacement leads to 8- and 4-fold decrease in the MICs of LVX and CIP, respectively, which is greater than that of Δ*mexB* or Δ*mexF* but not to the susceptible level of PAO1 (Fig 2 and S2 Table), suggesting that the target (*gyrA*) mutation also actively contributes to the FQ resistance in PA154197 and to a greater extent than drug efflux by MexAB-OprM or MexEF-OprN, but it does not mask the contribution of drug efflux.

316

317 **Exquisite resistance synergy shapes the MDR profile in PA154197.**

318 Previous investigations of resistance mechanisms by reconstitution in the laboratory model
319 strains [10, 38] is often incapable of revealing the relative contribution and synergy of multiple,
320 different resistance determinants owing to its susceptible strain background. The clinical MDR
321 strain PA154197 provides a paradigm to investigate these interactions. We first construct a
322 series of single, double and triple reverse mutations using the efficient editing technique
323 developed and examine the MIC of various antibiotics and antimicrobial agents in these strains
324 (Fig 2 and S2 Table). Our data above have shown that both drug efflux by the over-produced
325 MexAB-OprM and MexEF-OprN pumps and the *gyrA* target mutation contribute to FQ
326 resistance in PA154197 with *gyrA* mutations contributing to a greater extent of resistance than
327 drug efflux. Reverse of all three determinants (*gyrA*^{PAO1} *mexR*^{PAO1} *mexT*^{PAO1} strain) leads to
328 the complete loss of resistance to LVX and CIP, and an overall drug susceptibility in the strain
329 similar to PAO1, indicating these are the key resistant determinants of the MDR PA154197.
330 FICI values (0.156 for LVX and 0.047 for CIP) show that all three determinants synergize the
331 resistance to these two antipseudomonal FQs. Interestingly, MICs in the series of mutants
332 which harbour variable expression levels of efflux systems, i.e. over-production in the
333 PA154197 parent, basal level production in the strains of *mexR*^{PAO1} and *mexT*^{PAO1}, and no
334 production in the strains of Δ*mexB* and Δ*mexF*, reveals subtle differences of resistance
335 mechanisms between the two different FQ antibiotics by the interplay of the same set of
336 resistant determinants. For instance, while obvious and extensive synergy is observed in every
337 two combinations of *gyrA* mutation, MexAB over-production, and MexEF over-production for
338 CIP resistance, synergy between target (*gyrA*) mutation and drug efflux to confer LVX
339 resistance is observed when both the MexAB and MexEF pumps are over-produced as
340 evidenced by the FICI values calculated for LVX resistance in

gyrA^{PAO1}*mexR*^{PAO1}*mexF*^{PAO1}(0.156, synergy), *gyrA*^{PAO1}*mexR*^{PAO1} (1.125, indifference), and *gyrA*^{PAO1}*mexT* ^{PAO1} (1.125, indifference) (Fig 2). The drug target (*gyrA*) mutation dominates the LVX resistance when only one pump is over-produced.

In addition to FQs, over-production of the MexAB-OprM and MexEF-OprN pumps also synergize the resistance to the non-antipseudomonal antibiotics trimethoprim (TMP) and chloramphenicol (CHL) with an FICI value of 0.094 and 0.063, respectively. Resistance to antipseudomonal β-lactams including the penicillin-β-lactamase inhibitor combination is almost exclusively dependent on the activity of the MexAB-OprM pump in PA154197. Although mediated by the same resistance determinant, the efflux efficiency of different β-lactams by the same MexAB-OprM pump differs, with a greater extrusion efficiency observed for penicillins (CAR), monobactams (ATM), and penicillin-β-lactamase inhibitor combinations (TZP) than for cephalosporins (CAZ) and carbapenems (MEM) (Fig 2 and S3 Table). Notably, MICs of different β-lactams in *mexR*^{PAO1} relative to that in Δ*mexB* cells which reflect the efflux capacity of basal expression of MexAB-OprM (as the level in PAO1) reveals its high capacity of expelling penicillins (CAR) substrate (64 fold) and causing its resistance (S3 Table). MICs in the WT PA154197 relative to isogenic *mexR*^{PAO1} cells which reflects the efflux capacity contributed by over-production of MexAB-OprM reveals its extraordinary capacity of all β-lactams with the greatest extent of resistance enhancement observed in the case of monobactams ATM (16 fold) (S3 Table). The observed FQ resistance by MexAB-OprM is also contributed by its over-production (S3 Table). Combining these, a rather complete substrates profile of the two efflux pumps with relative expel efficiencies in the genetic background of the MDR strain PA154197 is mapped (Fig 5). This information not only advances our understanding of the relative contributions of resistance determinants and their interplay in the clinically isolated MDR strain PA154197 but also has implications in the clinical treatment of drug resistant infections.

366

367 **Lacking of collateral sensitivity in PA154197.**

368 It was proposed that resistance acquisition often leads to evolutionary trade-offs in resistant
369 strains, i.e. evolved resistance is costly in the absence of the drugs and leads to growth
370 deficiencies relative to the susceptible ancestor; or resistance mutations to one class of
371 antibiotics may exacerbate susceptibility against others, causing a phenomenon called
372 collateral sensitivity. Collateral sensitivity was first described as early as 1950s [47] and was
373 recently verified in a series of laboratory evolved resistant strains of *E. coli* and *P. aeruginosa*
374 [48-50]. It was proposed that collateral sensitivity is a common phenomenon in AMR strains
375 and can be exploited to eradicate clinical resistant strains or reduce resistance development by
376 programming the drug pairs that produce reciprocal collateral sensitivity [39, 51, 52]. However,
377 a recent study reported the lack of collateral sensitivity in clinical *P. aeruginosa* isolates from
378 the cystic fibrosis (CF) patients [53]. But the study did not investigate relative changes in strain
379 susceptibility due to the lack of appropriate baseline controls. The series of strains we
380 constructed which display variable level of resistance in the same genetic background of an
381 MDR strain allows investigating this phenomenon in the context of clinical MDR (a strain from
382 a blood stream infection). To address this, we measure the MICs of the two classes of
383 antibiotics the MDR strain PA154197 displays susceptibility: aminoglycosides (streptomycin
384 and gentamycin) and non-ribosomal peptides (Polymyxin B and colistin) and examine whether
385 the MDR PA154197 is more susceptible to these antibiotics than the series of isogenic, less-
386 resistant "ancestor" strains. However, it is shown that the strains containing various one or two
387 resistant determinants display the same level of susceptibility to aminoglycosides and
388 polymyxins with the WT which contains all three key resistant determinants (S2 Table).
389 Similar result is obtained in the susceptibility to another class of antibiotic which usually is not
390 used to treat *P. aeruginosa* infections, fosfomycin (FOF). These results suggest that unlike

391 those laboratory evolved strains with resistance to one or two specific classes of antibiotics,
392 clinical multidrug resistant strains perhaps have evolved compensatory mutations prevailing
393 the evolutionary trade-off of collateral sensitivity, rendering the treatment of MDR clinical
394 strains especially challenging.
395

396 ## Discussion

397 Emergence of resistance to multiple antimicrobial agents in pathogenic bacteria has become a
398 significant global public health threat as there are fewer, or even sometimes no, effective
399 antimicrobial agents to treat the infections caused by these bacteria. The MDR international
400 high-risk clones of *P. aeruginosa* are especially challenging in therapeutics owing to their
401 extraordinary drug resistance and rapid dissemination in hospitals worldwide [54-56]. Previous
402 molecular epidemic analyses have largely focused on identification of genetic variations in
403 resistant isolates in comparison with the model strain PAO1 [57]. To our knowledge, there has
404 been no systematic, functional genetics investigations of resistance development characterized
405 directly in the native genetic background of clinical MDR isolates. In this study, we report the
406 first single-plasmid-mediated, one-step genome editing technique applicable in the native
407 CRISPR-Cas containing, clinical *P. aeruginosa* strains, and its exploitation in MDR
408 characterization which provides new insight into the interplay and collateral effect of resistant
409 mutations in shaping the clinically significant MDR.
410 In comparison with a recently reported heterologous Cas9-based genome editing method which
411 requires successive transformation of two editing plasmids [35], and the conventional two-step
412 allelic exchange method [58] which takes more than two weeks to construct a mutant with an
413 undesirable FLP site permanently remained in the edited site, our method using a single
414 plasmid to achieve editing in one-step represents a more efficient and clean genome editing
415 technique which can be completed within one week, i.e. 3-4 days for constructing the editing

plasmid and 2-3 days for the luminescence-assisted selection and verification. The two-step In-Del strategy further developed to circumvent the limitation of poorly targeted genomic loci principally allows us to conduct any non-lethal genetic manipulation in the bacterial genome (Fig 6), greatly expanding and accelerating the molecular characterizations of the CRISPR-containing, MDR *P. aeruginosa* isolates. The methodology should be readily extended to other clinically significant pathogens, such as *Acinetobacter baumannii* and *Klebsiella spp*. to facilitate resistance characterization and management in these species.

Employing this powerful and efficient genome editing methodology, we not only verified the key resistant determinants but also revealed their relative contribution and interplay in shaping the MDR of the clinical strain PA154197 which are unable to be elucidated by reconstitution in the susceptible model strains. The G226T substitution in *mexR* is a newly identified point mutation occurred in PA154197 that leads to the de-repression of *mexAB-oprM*. Three resistant mutations are found to synergize FQ resistance, and mutations in *gyrA* elicit a greater extent of resistance than over-production of MexAB-OprM or MexEF-OprN. We speculate that the G226T mutation in *mexR* (leading to over-production of MexAB-OprM) and the target (*gyrA*) mutations were acquired after the *nfxC* type 8-bp deletion in *mexT* (leading to the over-production of MexEF-OprN and reduced production of OprD) as i) the *nfxC* type resistant strains often contain an impaired *mexAB-oprM* system and additional mutations are presumably needed to achieve simultaneous over-production of both MexEF-OprN and MexAB-OprM pumps; and ii) the contribution of drug efflux (by the MexEF-OprN) to resistance development is not only due to its direct expelling structurally diverse antibiotics but also the capability of driving the acquisition of additional, specific resistance mechanisms by lowering intracellular antibiotic concentration and promoting mutation accumulation [14, 59].

Lastly, we investigated the relative contributions, synergy, and collateral effects of different resistant determinants in conferring the resistance to different classes of antibiotics which

441 should have valuable implications in the treatment of clinical resistant strains. For instance,
442 given the substantial role of drug efflux in causing resistance to CAR, ATM, LVX, and CIP,
443 supplement of pump inhibitors with these antibiotics can conceivably improve the treatment of
444 infections caused by the MDR strain. Notably, studies carried out in a susceptible reference *P.*
445 *aeruginosa* strain and in *E. coli* showed no synergy between MexAB-OprM and MexEF-OprN
446 in expelling FQs [10]. In contrast to the observation in the laboratory evolved strains [39], no
447 collateral sensitivity and obvious evolution trade-offs such as growth defect in the absence of
448 antibiotics is observed in the clinical MDR strain PA154197. This discrepancy is likely due to
449 the genetic background of the clinical MDR strains and their extraordinary pathoadaptive
450 capabilities remain elucidated. These findings underlie the importance of investigating
451 resistance development in the native genetic background of resistant isolates.
452 Although genome sequencing and comparative genomics can identify the genetic variations in
453 resistance genes, whether and to what extent these variations contribute to the resistance
454 phenotype cannot be disclosed merely by genomic and transcriptome analyses. For instance,
455 we found that over-expression (~40-fold higher than in PAO1) of the efflux gene *mexH* and
456 nucleotide substitution in *parS* does not contribute to the drug resistance in PA154197. These
457 results suggest that not all genetic variations identified in resistance genes lead to the
458 development of antibiotic resistance, further highlighting the importance of the targeted
459 functional genomics investigations directly in the clinically isolated resistant strains.
460

461 # Material and methods

462 **Bacterial strains, culture conditions.**
463 All the bacterial strains used and constructed in this study are listed in S3 Table. *E. coli* DH5α
464 is used for plasmid construction and is usually cultured at 37°C in Luria-Bertani (LB) broth or
465 on the LB agar plate supplemented with 20 μg/ml Kanamycin (KAN). *P. aeruginosa*

PA154197 was isolated from the Queen Mary Hospital in Hong Kong, China [26]. PA154197 and its derivatives were selected in LB (broth or agar) with 500 μg/ml KAN at 37°C.

Plasmid construction.

All the plasmids constructed and used in this study are listed in S4 Table. Mini-CRISPR element consisting of two repeats flanking the PAM-protospacer was synthesized by BGI (Shenzhen, China). PCR was performed using the iProof™ High-Fidelity DNA Polymerase (Bio-Rad, USA). Mini-CRISPR elements and plasmid pAY5211 were digested using the restriction enzymes KpnI and BamHI (NEB, USA) and ligated using the Quick Ligation Kit (NEB, USA) to generate the targeting plasmid. Donor sequences which typically contain 500-bp upstream and 500-bp downstream of the editing sites were amplified by PCR and ligated into the linearized targeting plasmid (digested by XhoI (NEB, USA)) using the ClonExpress One Step Cloning Kit (Vazyme, China). All the constructed plasmids were verified by DNA sequencing (BGI, China).

Transformation of PA154197.

Electrocompetent PA154197 cells were prepared by firstly inoculating a fresh colony in LB broth and grown at 37°C overnight with 220-rpm agitation. Following subculture into 50 ml fresh LB broth and growing to OD_{600} = 0.5, cells were collected by centrifugation and washed three times with cold autoclaved Milli-Q H_2O. The resulting cells were resuspended into 1 ml Milli-Q H_2O. 100 μl electrocompetent PA154197 cells were then mixed with 1 μg editing plasmid and subject to electroporation (BTX, USA). 1 ml cold LB broth was added to recover the cells. Following culturing at 37°C for 1 h with agitation, cells were pelleted and resuspended in 100 μl LB for spreading (LB+KAN500). Transformants colonies were obtained after incubation at 37°C for 16-20 h.

Mutant screening and verification.

Colonies were firstly subjected to luminescence screening using the Synergy HTX Plate Reader (Bio Tek, USA). Colonies with high luminescent intensity were further verified by colony PCR using Taq DNA polymerase (Thermal Scientific, USA) with indicated primers and DNA sequencing (BGI, China). Sequencing results were visualized using DNA sequencing software Chromas (Technelysium Pty Ltd, Australia)

Curing of editing plasmid.

P. aeruginosa cells underwent one round of editing was streaked onto the LB ager plate and incubated at 37°C overnight. Single colony was selected and the curing was verified by the failure of growth in LB with 100 μg/ml KAN.

Minimum inhibitory concentration (MIC) measurement.

MIC was measured following the standard protocol of ASM with slight modification [60]. A single fresh colony of PA154197 was inoculated in LB medium overnight at 37°C with agitation. Overnight culture was then diluted to cell density of 10^5/ml, and 200 μl of the cells were distributed to each well of the 96-well plate. Antibiotics were then added with final concentrations ranging from 0.25 to 128 μg/ml. Plates were incubated at 37°C for 16-20 h and MIC value was determined by absorbance at 600 nm.

Reverse transcription (RT)-quantitative PCR (qPCR).

Bacterial cells from overnight culture were harvested by centrifugation at 4°C. Total RNA was extracted using RNeasy Mini Kit (Qiagen, Germany) according to the manufacturer's instruction. Reverse transcription was performed using PrimeScript RT reagent Kit (Takara,

Japan). qPCR was performed using specific primers and the SYBR Green PCR master mix (Applied Biosystems, USA) in a 20 µl reaction system. The reaction was performed in ABI StepOnePlus real time PCR system with *recA* and *clpX* as reference genes to normalize the relative expression of the target genes. The results were expressed as fold change of the expression of target genes, and results were presented as the mean of three independent biological isolates.

Disk diffusion assay.

20 µl overnight culture as described above was mixed with 5 ml melted LB top agar (0.75 %) and poured on a LB agar plate. After the agar was solidified, round filter paper disks were placed. 5µl antibiotic solution (2 mg/ml) was added to the centre of the paper disks. The plates were incubated at 37°C for 16 h.

Fractional inhibitory concentration index (FICI) determination.

Synergy of mutation combinations was determined using the FICI method [39]. The MIC of the mutant with combined mutations is divided by the MICs of the mutants with single mutation, yielding the fractional contribution of each mutation in the combination. Interaction of different mutations (A, B, C) is scored using the following formula: $FICI_{(ABC)}=MIC_{(ABC)}/MIC_{(A)}+ MIC_{(ABC)}/MIC_{(B)}+ MIC_{(ABC)}/MIC_{(C)}$.

Acknowledgements

We thank Prof. Susumu Yoshizawa and Prof. Kazuhiro Kogure (Both from the University of Tokyo) for sharing the ocean-100 strain. We appreciate Dr. Xin Deng (Department of Biomedical Sciences, City University of Hong Kong) for the pMS402 vector and Dr. Zhaoxun

Liang (School of Biological Sciences, Nanyan Technological University, Singapore) for his advice on the manuscript writing.

References

1. Oliver A, Mulet X, López-Causapé C, Juan C. The increasing threat of *Pseudomonas aeruginosa* high-risk clones. Drug Resist Updates. 2015;21:41-59. doi: 10.1016/j.drup.2015.08.002 PMID: 26304792
2. Stover CK, Pham XQ, Erwin A, Mizoguchi S, Warrener P, Hickey M, et al. Complete genome sequence of *Pseudomonas aeruginosa* PAO1, an opportunistic pathogen. Nature. 2000;406(6799):959-964. doi: 10.1038/35023079 PMID: 10984043
3. Poole K. *Pseudomonas aeruginosa*: resistance to the max. Front Microbiol. 2011;2:65. doi:10.3389/fmicb.2011.00065 PMID: 21747788
4. Santajit S, Indrawattana N. Mechanisms of antimicrobial resistance in ESKAPE pathogens. BioMed Res Int. 2016;2016: 2475067. doi: 10.1155/2016/2475067 PMID: 27274985
5. Magiorakos AP, Srinivasan A, Carey R, Carmeli Y, Falagas M, Giske C, et al. Multidrug-resistant, extensively drug-resistant and pandrug-resistant bacteria: an international expert proposal for interim standard definitions for acquired resistance. Clin Microbiol Infect. 2012;18(3):268-281. doi: 10.1111/j.1469-0691.2011.03570.x PMID: 21793988
6. Hocquet D, Berthelot P, Roussel-Delvallez M, Favre R, Jeannot K, Bajolet O, et al. *Pseudomonas aeruginosa* may accumulate drug resistance mechanisms without losing its ability to cause bloodstream infections. Antimicrob Agents Chemother. 2007;51(10):3531-3536. doi: 10.1128/AAC.00503-07 PMID: 17682106
7. Cabot G, Ocampo-Sosa AA, Dominguez MA, Gago JF, Juan C, Tubau F, et al. Genetic markers of widespread extensively drug-resistant *Pseudomonas aeruginosa* high-risk

564 clones. Antimicrob Agents Chemother. 2012;56(12):6349-6357. doi:
565 10.1128/AAC.01388-12 PMID: 23045355

566 8. Hocquet D, Bertrand X, Kohler T, Talon D, Plesiat P. Genetic and phenotypic variations
567 of a resistant *Pseudomonas aeruginosa* epidemic clone. Antimicrob Agents Chemother.
568 2003;47(6):1887-1894. doi: 10.1128/AAC.47.6.1887-1894.2003 PMID: 12760863

569 9. Köhler T, Epp SF, Curty LK, Pechère J-C. Characterization of MexT, the regulator of the
570 MexE-MexF-OprN multidrug efflux system of *Pseudomonas aeruginosa*. J Bacteriol.
571 1999;181(20):6300-6305. PMID: 10515918

572 10. Bruchmann S, Dötsch A, Nouri B, Chaberny IF, Häussler S. Quantitative contribution of
573 target alteration and decreased drug accumulation to *Pseudomonas aeruginosa*
574 fluoroquinolone resistance. Antimicrob Agents Chemother. 2012;57(3):1361-1368. doi:
575 10.1128/AAC.01581-12 PMID: 23274661

576 11. Riera E, Cabot G, Mulet X, Garcia-Castillo M, del Campo R, Juan C, et al. *Pseudomonas*
577 *aeruginosa* carbapenem resistance mechanisms in Spain: impact on the activity of
578 imipenem, meropenem and doripenem. J Antimicrob Chemother. 2011;66(9):2022-2027.
579 doi: 10.1093/jac/dkr232 PMID: 21653605.

580 12. Llanes C, Hocquet D, Vogne C, Benali-Baitich D, Neuwirth C, Plesiat P. Clinical strains
581 of *Pseudomonas aeruginosa* overproducing MexAB-OprM and MexXY efflux pumps
582 simultaneously. Antimicrob Agents Chemother. 2004;48(5):1797-802. doi:
583 10.1128/AAC.48.5.1797-1802.2004 PMID: 15105137

584 13. Horna G, Lopez M, Guerra H, Saenz Y, Ruiz J. Interplay between MexAB-OprM and
585 MexEF-OprN in clinical isolates of *Pseudomonas aeruginosa*. Sci Rep. 2018;8(1):16463.
586 doi: 10.1038/s41598-018-34694-z PMID: 30405166

14. Li XZ, Plesiat P, Nikaido H. The challenge of efflux-mediated antibiotic resistance in Gram-negative bacteria. Clin Microbiol Rev. 2015;28(2):337-418. doi: 10.1128/CMR.00117-14 PMID: 25788514

15. Lee A, Mao WM, Warren MS, Mistry A, Hoshino K, Okumura R, et al. Interplay between efflux pumps may provide either additive or multiplicative effects on drug resistance. J Bacteriol. 2000;182(11):3142-3150. doi:10.1128/jb.182.11.3142-3150.2000 PMID: 10809693

16. Mulet X, Moyá B, Juan C, Macià MD, Pérez JL, Blázquez J, et al. Antagonistic interactions of *Pseudomonas aeruginosa* antibiotic resistance mechanisms in planktonic but not biofilm growth. Antimicrob Agents Chemother. 2011;55(10):4560-4568. doi: 10.1128/AAC.00519-11 PMID: 21807976

17. Maseda H, Sawada I, Saito K, Uchiyama H, Nakae T, Nomura NJAa, et al. Enhancement of the *mexAB-oprM* efflux pump expression by a quorum-sensing autoinducer and its cancellation by a regulator, MexT, of the *mexEF-oprN* efflux pump operon in *Pseudomonas aeruginosa*. Antimicrob Agents Chemother. 2004;48(4):1320-1328. doi: 10.1128/AAC.48.4.1320-1328.2004 PMID: 15047536

18. Vogwill T, Kojadinovic M, MacLean RC. Epistasis between antibiotic resistance mutations and genetic background shape the fitness effect of resistance across species of *Pseudomonas*. Proc Biol Sci. 2016;283(1830). doi: 10.1098/rspb.2016.0151 PMID: 27170722

19. de Sousa JM, Balbontín R, Durão P, Gordo I. Multidrug-resistant bacteria compensate for the epistasis between resistances. PLoS Biol. 2017;15(4):e2001741. doi: 10.1371/journal.pbio.2001741 PMID: 28419091

610 20. Vogwill T, Kojadinovic M, Furio V, MacLean RC. Testing the role of genetic background
611 in parallel evolution using the comparative experimental evolution of antibiotic resistance.
612 Mol Biol Evol. 2014;31(12):3314-23. doi: 10.1093/molbev/msu262 PMID: 25228081

613 21. van Belkum A, Soriaga LB, LaFave MC, Akella S, Veyrieras J-B, Barbu EM, et al.
614 Phylogenetic distribution of CRISPR-Cas systems in antibiotic-resistant *Pseudomonas*
615 *aeruginosa*. MBio. 2015;6(6):e01796-15. doi: 10.1128/mBio.01796-15 PMID: 26604259
616 22. Cheng F, Gong L, Zhao D, Yang H, Zhou J, Li M, et al. Harnessing the native type IB
617 CRISPR-Cas for genome editing in a polyploid archaeon. J Genet Genomics.
618 2017;44(11):541-548. doi: 10.1016/j.jgg.2017.09.010 PMID: 29169919
619 23. Zhang J, Zong W, Hong W, Zhang Z-T, Wang Y. Exploiting endogenous CRISPR-Cas
620 system for multiplex genome editing in *Clostridium tyrobutyricum* and engineer the strain
621 for high-level butanol production. Metab Eng. 2018;47:49-59. doi:
622 10.1016/j.ymben.2018.03.007 PMID: 29530750
623 24. Li Y, Pan S, Zhang Y, Ren M, Feng M, Peng N, et al. Harnessing Type I and Type III
624 CRISPR-Cas systems for genome editing. Nucleic Acids Res. 2015;44(4):e34-e. doi:
625 10.1093/nar/gkv1044 PMID: 26467477
626 25. Pyne ME, Bruder MR, Moo-Young M, Chung DA, Chou CP. Harnessing heterologous and
627 endogenous CRISPR-Cas machineries for efficient markerless genome editing in
628 *Clostridium*. Sci Rep. 2016;6:25666. doi: 10.1038/srep25666 PMID: 27157668
629 26. Cao H, Xia T, Li Y, Bougouffa S, Lo YK, Bajic VB, et al. A multidrug resistant clinical *P.*
630 *aeruginosa* isolate in the MLST550 clonal complex: uncoupled quorum sensing modulates
631 the interplay of virulence and resistance. bioRxiv. 2018. doi:
632 https://doi.org/10.1101/415000

633 27. Yonezawa M, Takahata M, Matsubara N, Watanabe Y, Narita H. DNA gyrase *gyrA*
634 mutations in quinolone-resistant clinical isolates of *Pseudomonas aeruginosa*. Antimicrob
635 Agents Chemother. 1995;39(9):1970-1972. doi: 10.1128/AAC.39.9.1970 PMID: 8540700
636 28. Juan C, Maciá MD, Gutiérrez O, Vidal C, Pérez JL, Oliver A. Molecular mechanisms of β-
637 lactam resistance mediated by AmpC hyperproduction in *Pseudomonas aeruginosa* clinical
638 strains. Antimicrob Agents Chemother. 2005;49(11):4733-4738. doi:
639 10.1128/AAC.49.11.4733-4738.2005 PMID: 16251318
640 29. Richter C, Gristwood T, Clulow JS, Fineran PC. In vivo protein interactions and complex
641 formation in the *Pectobacterium atrosepticum* subtype IF CRISPR/Cas System. PLoS One.
642 2012;7(12):e49549. doi: 10.1371/journal.pone.0049549 PMID: 23226499
643 30. Cady KC, Bondy-Denomy J, Heussler GE, Davidson AR, O'Toole GA. The CRISPR/Cas
644 adaptive immune system of *Pseudomonas aeruginosa* mediates resistance to naturally
645 occurring and engineered phages. J Bacteriol. 2012;194(21):5728-5738. doi:
646 10.1128/JB.01184-12 PMID: 22885297
647 31. Leenay RT, Beisel CL. Deciphering, communicating, and engineering the CRISPR PAM.
648 J Mol Biol. 2017;429(2):177-191. doi: 10.1016/j.jmb.2016.11.024 PMID: 27916599
649 32. Olsen RH, DeBusscher G, McCombie WR. Development of broad-host-range vectors and
650 gene banks: self-cloning of the *Pseudomonas aeruginosa* PAO chromosome. J Bacteriol.
651 1982;150(1):60-69. PMID: 6277872
652 33. Shah NCM. Construction and development of bioluminescent *Pseudomonas aeruginosa*
653 strains; application in biosensors for preservative efficacy testing. PhD Thesis, University
654 of Hertfordshire. 2014. Available from: https://uhra.herts.ac.uk/handle/2299/15592
655 34. Xu L, Chen H, Hu XH, Zhang RM, Zhang Z, Luo ZW. Average gene length is highly
656 conserved in prokaryotes and eukaryotes and diverges only between the two kingdoms.
657 Mol Biol Evol. 2006;23(6):1107-1108. doi: 10.1093/molbev/msk019 PMID: 16611645

658 35. Chen W, Zhang Y, Zhang Y, Pi Y, Gu T, Song L, et al. CRISPR/Cas9-based genome
659 editing in *Pseudomonas aeruginosa* and cytidine deaminase-mediated base editing in
660 *Pseudomonas* species. iScience. 2018;6:222-231. doi: 10.1016/j.isci.2018.07.024 PMID:
661 30240613
662 36. Chen W, Zhang Y, Yeo W-S, Bae T, Ji Q. Rapid and efficient genome editing in
663 *Staphylococcus aureus* by using an engineered CRISPR/Cas9 system. J Am Chem Soc.
664 2017;139(10):3790-3795. doi: 10.1021/jacs.6b13317 PMID: 28218837
665 37. Kumagai Y, Yoshizawa S, Nakamura K, Ogura Y, Hayashi T, Kogure K. Complete and
666 draft genome sequences of eight oceanic pseudomonas aeruginosa strains. Genome
667 Announc. 2017;5(44):e01255-17. doi: 10.1128/genomeA.01255-17 PMID: 29097479
668 38. Köhler T, Michéa-Hamzehpour M, Henze U, Gotoh N, Kocjancic Curty L, Pechère JC.
669 Characterization of MexE–MexF–OprN, a positively regulated multidrug efflux system of
670 *Pseudomonas aeruginosa*. Mol Microbiol. 1997;23(2):345-354. PMID: 9044268
671 39. Gonzales PR, Pesesky MW, Bouley R, Ballard A, Biddy BA, Suckow MA, et al.
672 Synergistic, collaterally sensitive β-lactam combinations suppress resistance in MRSA. Nat
673 Chem Biol. 2015;11(11):855-861. doi: 10.1038/nchembio.1911 PMID: 26368589
674 40. Sánchez P, Rojo F, Martínez JL. Transcriptional regulation of *mexR*, the repressor of
675 *Pseudomonas aeruginosa mexAB-oprM* multidrug efflux pump. FEMS Microbiol Lett.
676 2002;207(1):63-68. doi: 10.1111/j.1574-6968.2002.tb11029.x PMID: 11886752
677 41. Adewoye L, Sutherland A, Srikumar R, Poole K. The *mexR* repressor of the *mexAB-oprM*
678 multidrug efflux operon in *Pseudomonas aeruginosa*: characterization of mutations
679 compromising activity. J Bacteriol. 2002;184(15):4308-4312. doi:
680 10.1128/JB.184.15.4308-4312.2002 PMID: 12107151
681 42. Saito K, Yoneyama H, Nakae T. *nalB*-type mutations causing the overexpression of the
682 MexAB-OprM efflux pump are located in the *mexR* gene of the *Pseudomonas aeruginosa*

683 chromosome. FEMS Microbiol Lett. 1999;179(1):67-72. doi: 10.1111/j.1574-
684 6968.1999.tb08709.x PMID: 10481088
685 43. Maseda H, Saito K, Nakajima A, Nakae T. Variation of the *mexT* gene, a regulator of the
686 MexEF-OprN efflux pump expression in wild-type strains of *Pseudomonas aeruginosa*.
687 FEMS Microbiol Lett. 2000;192(1):107-112. doi: 10.1111/j.1574-6968.2000.tb09367.x
688 PMID: 11040437
689 44. Linares JF, López JA, Camafeita E, Albar JP, Rojo F, Martínez JLJJob. Overexpression of
690 the multidrug efflux pumps MexCD-OprJ and MexEF-OprN is associated with a reduction
691 of type III secretion in *Pseudomonas aeruginosa*. J Bacteriol. 2005;187(4):1384-1391. doi:
692 10.1128/JB.187.4.1384-1391.2005 PMID: 15687203
693 45. Wang D, Seeve C, Pierson LS, Pierson EA. Transcriptome profiling reveals links between
694 ParS/ParR, MexEF-OprN, and quorum sensing in the regulation of adaptation and
695 virulence in *Pseudomonas aeruginosa*. BMC Genomics. 2013;14:618. doi: 10.1186/1471-
696 2164-14-618 PMID: 24034668
697 46. Varughese LR, Rajpoot M, Goyal S, Mehra R, Chhokar V, Beniwal V. Analytical profiling
698 of mutations in quinolone resistance determining region of *gyrA* gene among UPEC. PloS
699 one. 2018;13(1):e0190729. doi: 10.1371/journal.pone.0190729 PMID: 29300775
700 47. Szybalski W, Bryson VJJob. Genetic studies on microbial cross resistance to toxic agents
701 i.: cross resistance of *Escherichia coli* to fifteen antibiotics. J Bacteriol. 1952;64(4):489-
702 499. PMID: 12999676
703 48. Pál C, Papp B, Lázár VJTim. Collateral sensitivity of antibiotic-resistant microbes. Trends
704 Microbiol. 2015;23(7):401-407. doi: 10.1016/j.tim.2015.02.009 PMID: 25818802
705 49. Barbosa C, Trebosc V, Kemmer C, Rosenstiel P, Beardmore R, Schulenburg H, et al.
706 Alternative evolutionary paths to bacterial antibiotic resistance cause distinct collateral

effects. Mol Biol Evol. 2017;34(9):2229-2244. doi: 10.1093/molbev/msx158 PMID: 28541480

50. Podnecky NL, Fredheim EG, Kloos J, Sørum V, Primicerio R, Roberts AP, et al. Conserved collateral antibiotic susceptibility networks in diverse clinical strains of *Escherichia coli*. Nat Commun. 2018;9(1):3673. doi: 10.1038/s41467-018-06143-y PMID: 30202004
51. Wambaugh MA, Shakya VP, Lewis AJ, Mulvey MA, Brown JCS. High-throughput identification and rational design of synergistic small-molecule pairs for combating and bypassing antibiotic resistance. PLoS Biol. 2017;15(6):e2001644. doi: 10.1371/journal.pbio.2001644 PMID: 28632788
52. Lázár V, Martins A, Spohn R, Daruka L, Grézal G, Fekete G, et al. Antibiotic-resistant bacteria show widespread collateral sensitivity to antimicrobial peptides. Nat Microbiol. 2018;3(6):718-731. doi: 10.1038/s41564-018-0164-0 PMID: 29795541
53. Jansen G, Mahrt N, Tueffers L, Barbosa C, Harjes M, Adolph G, et al. Association between clinical antibiotic resistance and susceptibility of *Pseudomonas* in the cystic fibrosis lung. Evol Med Public Health. 2016;2016(1):182-94. doi: 10.1093/emph/eow016 PMID: 27193199
54. Breidenstein EB, de la Fuente-Núñez C, Hancock RE. *Pseudomonas aeruginosa*: all roads lead to resistance. Trends Microbiol. 2011;19(8):419-426. doi: 10.1016/j.tim.2011.04.005 PMID: 21664819
55. Cheng VC, Wong SC, Ho P-L, Yuen K-Y. Strategic measures for the control of surging antimicrobial resistance in Hong Kong and mainland of China. Emerg Microbes Infect. 2016;4(2):e8. doi: 10.1038/emi.2015.8 PMID: 26038766
56. Wright GD. Antibiotic adjuvants: rescuing antibiotics from resistance. Trends Microbiol. 2016;24(11):862-871. doi: 10.1016/j.tim.2016.06.009 PMID: 27430191

731 57. Jia B, Raphenya AR, Alcock B, Waglechner N, Guo P, Tsang KK, et al. CARD 2017:
732 expansion and model-centric curation of the comprehensive antibiotic resistance database.
733 Nucleic Acids Res. 2016;45(D1):D566-D573. doi: 10.1093/nar/gkw1004 PMID: 27789705
734 58. Choi K-H, Schweizer HP. An improved method for rapid generation of unmarked
735 *Pseudomonas aeruginosa* deletion mutants. BMC Microbiol. 2005;5(1):30. doi:
736 10.1186/1471-2180-5-30 PMID: 15907219
737 59. Sun J, Deng Z, Yan A. Bacterial multidrug efflux pumps: mechanisms, physiology and
738 pharmacological exploitations. Biochem Biophys Res Commun. 2014;453(2):254-267. doi:
739 10.1016/j.bbrc.2014.05.090 PMID: 24878531
740 60. Coyle MB et al. Manual of Antimicrobial Susceptibility Testing. American Society for
741 Microbiology; 2005.

742

743

Figure captions

Fig 1. Repurposing the functional native CRISPR-Cas system for gene deletion. (A) Schematic representation of the native type I-F CRISPR-Cas in PA154197. Diamonds and rectangles indicate the repeat and spacer units of a CRISPR array, respectively. Curved arrows (in black) above the leader sequence (in brown) indicate the orientation of CRISPR transcription. The consensus repeat of the two CRISPR arrays differs by one nucleotide (in red). **(B)** Schematic showing the design of the *mexB*-targeting plasmid (pAY5233) and the *mexB*-deletion donor. The mini-CRISPR in pAY5233 comprises a 32-bp spacer (in blue) targeting the *mexB* gene and two flanking repeats (in yellow), and is co-expressed with the reporter *lux* operon (in green) under the control of the strong promoter P*tat*. The PAM sequence is framed. The donor (in pink) consists of sequences upstream (U1) and downstream (D1) of *mexB*. The *Kpn*I and *BamH*I sites are used for mini-CRISPR insertion and the *Xho*I site is used for one-step cloning of the donor. **(C)** Representative plates showing the transformation efficiency of the vector control pAY5211, the targeting plasmid pAY5233, and the editing plasmid pAY5235. **(D)** Design of the *mexB*-deletion plasmid pAY5235 which contains both the self-targeting CRISPR and the repair donor. **(E)** Eight randomly selected transformants were subjected to colony PCR to screen for the Δ*mexB* mutants (positive clones are highlighted in red). Primers used in colony PCR (F1/R1) are indicated in panel (B). **(F)** The screened Δ*mexB* mutants in (E) were further validated by DNA sequencing.

Fig 2. MIC fold-change of various antimicrobial agents in PA154197 isogenic mutants and FICI profiling of reverse mutation combinations. MICs of 12 antimicrobial agents (8 antipseudomonal antibiotics and 4 other antimicrobial agents) were tested in 12 PA154197 isogenic mutants. MIC fold-changes between the wild-type PA154197 and mutants are expressed by the color key shown (detailed MIC values are shown in S2 Table). FICI profiles

of various mutation combinations against different antimicrobial agents are presented. FICI values below 0.5 which indicates synergy are highlighted in orange.

Fig 3. Expression levels of the *mexAB*, *mexEF* and *oprD* genes in PAO1, PA154197 and its isogenic mutants *mexR*^{PAO1} *mexT*^{PAO1}. (A) Schematic showing the regulation of *mexAB-oprM*, *mexEF-oprN* and *oprD* in *P. aeruginosa*. MexR represses the expression of *mexAB-oprM*; MexT activates *mexEF-oprN* and represses *oprD*. **(B)** Transcription alteration of *mexA* and *mexB* in PA154197 and in PAO1, and in PA154197 and its isogenic *mexR*^{PAO1} mutant. **(C)** Transcription alteration of *mexE*, *mexF* and *oprD* in PA154197 and in PAO1, and in PA154197 and its isogenic *mexT*^{PAO1} mutant.

Fig 4. The two-step In-Del editing strategy (taking insertion of 8 bp into *mexT* as an example). (A) Schematic design of the two-step In-Del method. In the first step, a 32-bp exogenous DNA sequence (tag, in pink) is introduced to an auxiliary target site (in blue), between its PAM and protospacer portions. In the second step, a tag-targeting CRISPR, as well as a tag-lacking donor which contains the desired mutation (8-bp insertion in this case), is provided to simultaneously remove the exogenous tag and achieve the desired mutation. **(B)** Randomly selected luminescence positive colonies from the two steps were subjected to colony PCR using the primers F2/Seq-R2 (indicated in panel A). Desired mutants are highlighted in red. **(C)** Targets in the potential mutants from the two steps were amplified using the primers Seq-F2/Seq-R2 (indicated in panel A) and validated by DNA sequencing. Representative DNA sequencing results from the two steps are shown, where the tag sequence is shown in pink.

Fig 5. Substrates profile and their relative efflux efficiency by the over-produced MexAB-OprM and MexEF-OprN systems in PA154197. Substrate profiles of the MexAB-OprM and

MexEF-OprN and their preferences are shown schematically based on the MIC alterations (Fig 2 and S2 Table) in the Δ*mexB*, Δ*mexF*, and Δ*mexB* Δ*mexF* cells relative to the WT. The greater the MIC changes in the single mutant relative to the WT, the stronger substrates they are denoted. The strength of the substrate preference is expressed by the color key shown, except for the TMP, CHL and FOF (in grey) which MICs were only changed in the double mutant.

Fig 6. Schematic diagram of the native type I-F CRISPR-Cas mediated genome editing in PA154197 and its exploitations in functional genomics investigation. Desired mutants with altered resistance (or virulence, other physiology) can be obtained in one step by introducing a programmable editing plasmid, which carries a mini-CRISPR (expressing a crRNA) and a repair donor, into the MDR/XDR PA154197 cells with ready luminescence selection. The crRNA directs the Cascade complex to the target. Recombination occurs between the repair donor and the target area to prevent the target interference, resulting in the desired mutation. Two-step editing can be utilized to obtain mutations in the genetic loci that cannot be well targeted by CRISPR. The red sequence indicates a resistant determinant (target) in PA154197. Cells containing the editing plasmid expressing the *lux* genes are shown in green.

Supporting information

S1 Fig. Effect of desired truncation lengths on the efficiency of editing. (A) Schematic diagram of the genetic locus of *mexB* and adjacent region. Desired truncation fragments of 50 bp (B1, 74-123), 500 bp (B2, 74-573), 1000 bp (B3, 74-1073), the full length (*mexB*, 1-3141), and the primers to test these truncations are shown. **(B)** Positive clones of each of truncations in eight randomly selected transformants are highlighted in red.

S2 Fig. Curing of the editing plasmid in the edited cells. Edited cells could not grow in the presence of kanamycin (100 μg/ml) after plasmid curing, which was achieved by culturing the edited cells without antibiotic pressure overnight.

S3 Fig. Harnessing the native type I-F CRISPR-Cas system for genome editing in other *P. aeruginosa* isolates. The single editing plasmid pAY5235 was transformed in the clinical *P. aeruginosa* isolate PA150567 and the environmental isolate Ocean-100 to achieve *mexB* deletion in one-step. Eight randomly selected luminescent transformants were subjected to colony PCR to screen for the desired Δ*mexB* mutants. Positive clones are highlighted in red. Primers used in colony PCR are indicated in Figure 1B.

S4 Fig. Disk diffusion assay of the antibiotic susceptibilities of PA154197 and its isogenic mutants. Disk diffusion test is conducted to examine the susceptibility of PA154197 and its isogenic mutants to eight antipseudomonal drugs **(A)** and four other antibiotics and antimicrobial agents **(B)**. Larger inhibition zone represents the higher susceptibility to the indicated antibiotics.

S5 Fig. Growth curves of PA154197 and its isogenic mutants in the absence of antibiotics.

836 No difference of growth among PA154197 and its isogenic mutants were observed.

837

838 **S6 Fig. Depiction of genetic mutations identified in the key antibiotic resistance genes**
839 ***mexR*, *mexT* and GyrA in PA154197. (A)** The point mutation (G226T) in PA154197 *mexR*
840 gene leads to premature termination of its protein product. **(B)** An 8-bp deletion in PA154197
841 *mexT* relative to that in PAO1 converts the out-of-frame *mexT* product to the in-frame, active
842 form of *mexT* product. **(C)** PA154197 *gyrA* gene contains a T248C substitution (corresponding
843 to T83I in the GyrA protein) in the quinolone resistance-determining region (QRDR) and a
844 ^{2723}CCGAGT^{2728} 6-bp deletion (corresponding to the deletion of E959&S960) in the C terminal
845 domain of the gene product.

846

847 **S7 Fig. Non-efficient targeting at the desired editing site in the *mexT* gene. (A)** Schematic
848 showing the desired 8-bp insertion (CGGCCAGC) into the *mexT* gene. The 6-bp repeat
849 sequences (in red) in the target which potentially obscure the targeting by the CRISPR-Cas
850 apparatus are shown. PAM is shown in frame. **(B)** No desirable DNA interference was observed
851 by transforming the *mexT*-targeting plasmid pAY5900 into PA154197 cells in comparison with
852 the control plasmid pAY5211. Note that no repair donor was provided in this plasmid.

853

854 **S8 Fig. Replacing the essential gene *gyrA* with that from PAO1 using the two-step In-Del**
855 **method. (A)** Schematic showing the two-step strategy for *gyrA* gene replacement. The tag
856 sequence (in pink) is first introduced downstream of *gyrA* (in orange) between the PAM and
857 protospacer portions of a selected target (in blue). In the second step, a tag-targeting plasmid
858 carrying the repair donor (Del-donor) is provided. Del-donor lacks the tag sequence but
859 contains the *gyrA* gene (in dark blue) from PAO1, which is flanked by two ~1000-bp sequences
860 upstream and downstream of the PA154197 *gyrA* gene. The primer pairs F/Seq-R and Seq-

F/Seq-R were used for the colony PCR analysis in (B) and DNA sequencing, respectively. **(B)** Eight luminescent positive transformants from each editing step were randomly selected for colony PCR analysis. Desired mutants confirmed by DNA sequencing are highlighted in red.

S1 Table. A summary of mutational changes in the antibiotic resistance (AR) genes in PA154197 by comparative genomic analysis

S2 Table. MICs of various antibiotics in PAO1, PA154197 and its isogenic mutants

S3 Table. Contribution of basal-level, over-produced and overall MexAB-OprM pump to the resistance to different antipseudomonal antibiotics in PA154197

S4 Table. Bacterial strains, plasmids used in this study

875 **Fig 1**

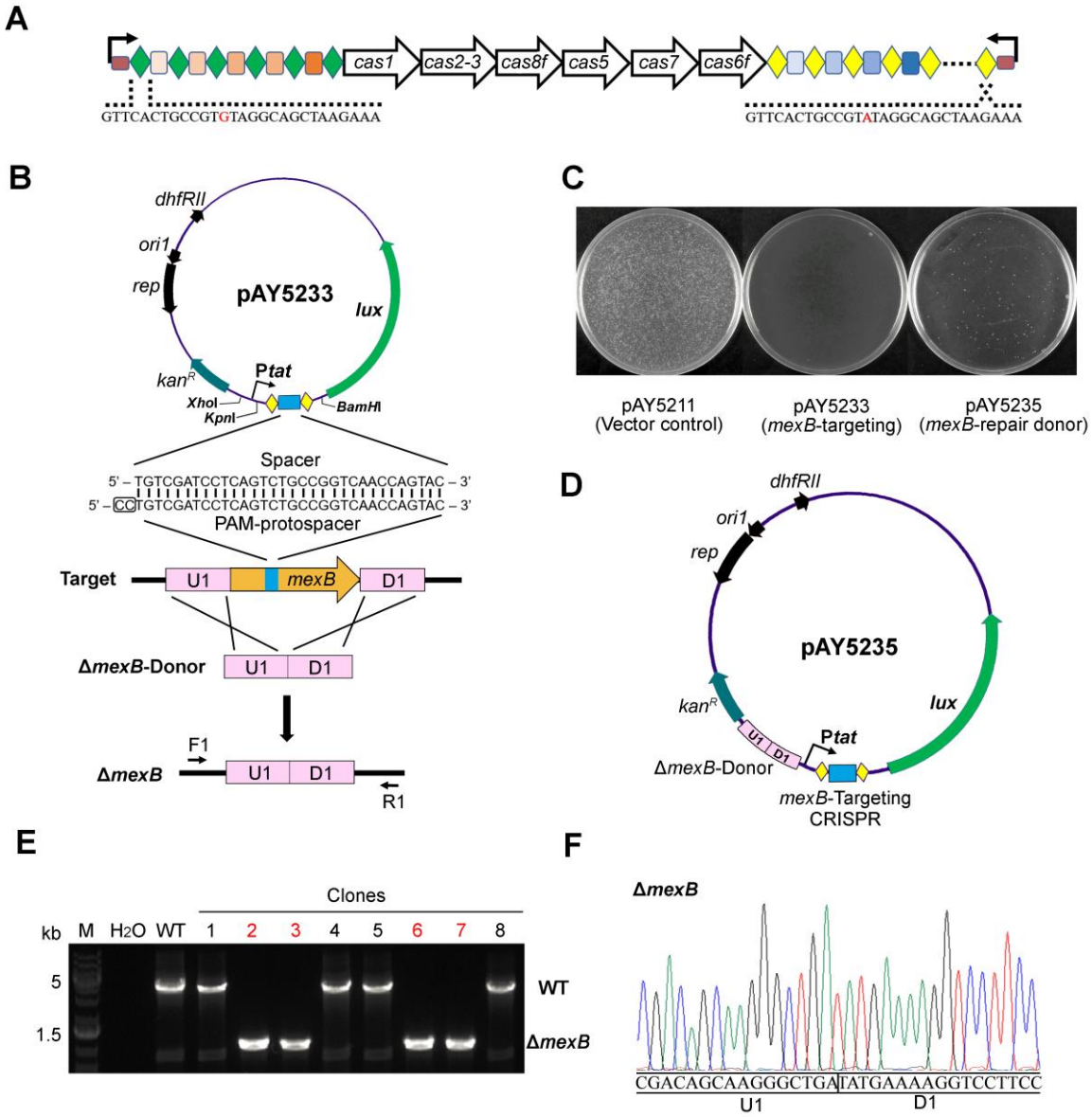

876

877

878 **Fig 2**

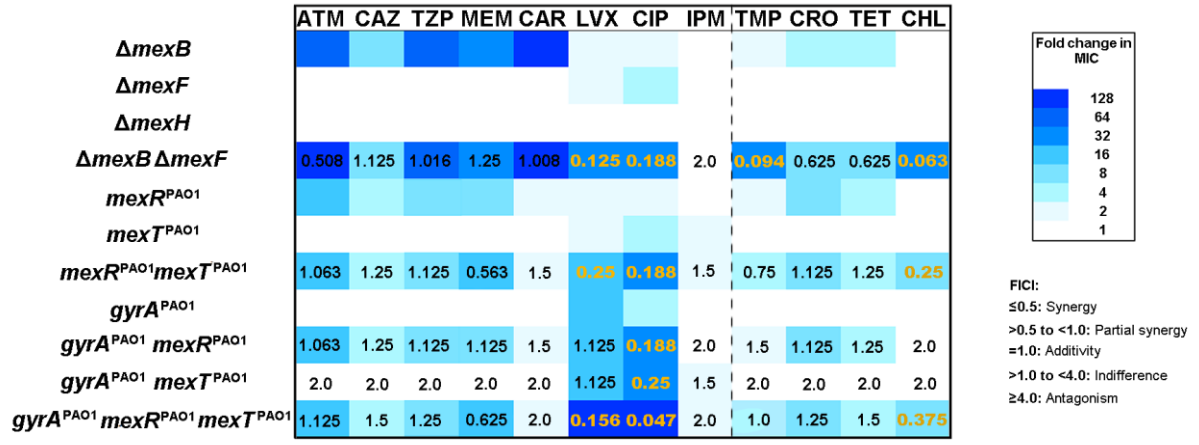

Antipseudomonal antibiotics: ATM: Aztreonam; **CAZ:** Ceftazidime; **TZP:** piperacillin-tazobactam; **MEM:** Meropenem; **CAR:** Carbenicillin; **LVX:** Levofloxacin; **CIP:** Ciprofloxacin; **IPM:** Imipenem
Other antibmicrobial agents: TMP: Trimethoprim; **CRO:** Ceftriaxone; **TET:** Tetracycline; **CHL:** Chloramphenicol

879

880

881 **Fig 3**

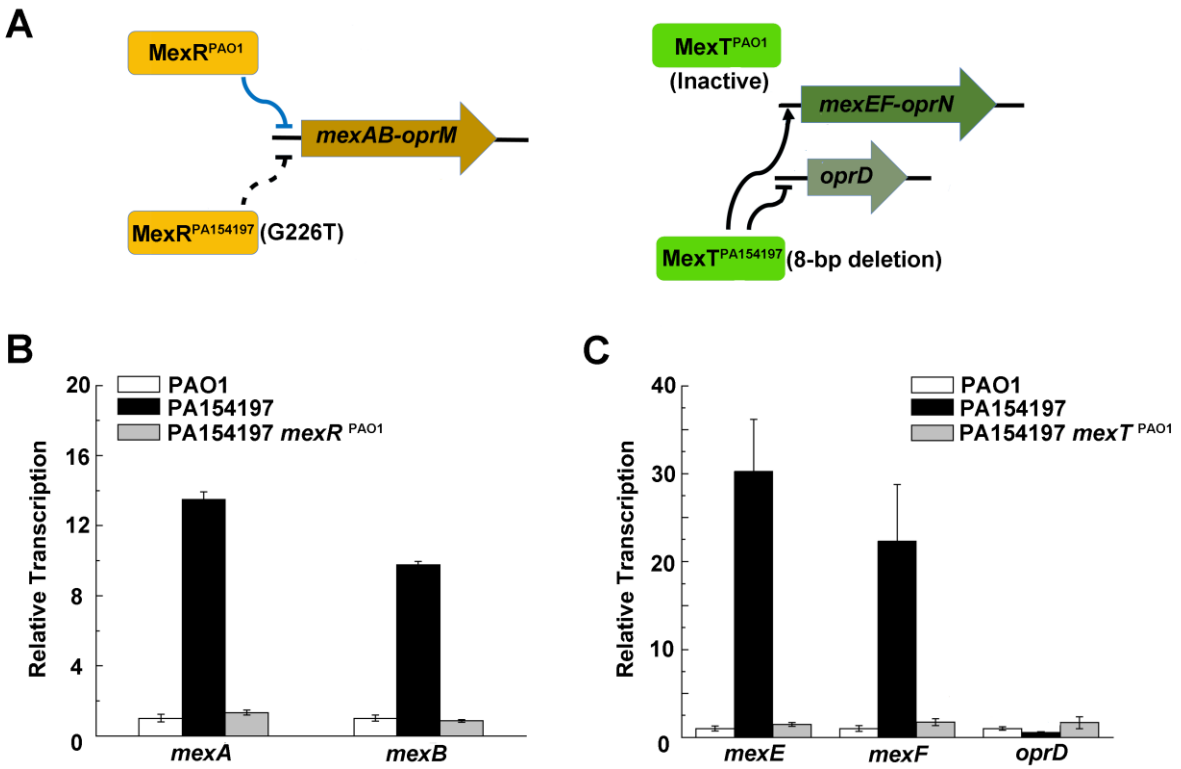

882

883

884 **Fig 4**

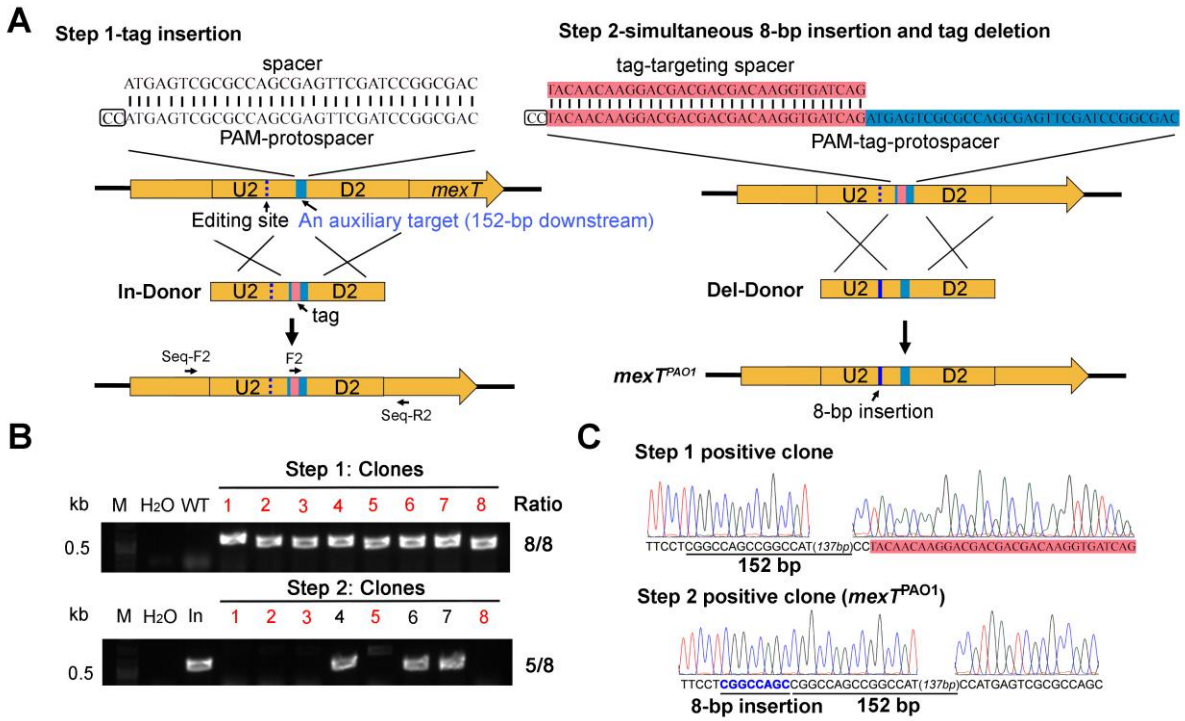

885

886

887 **Fig 5**

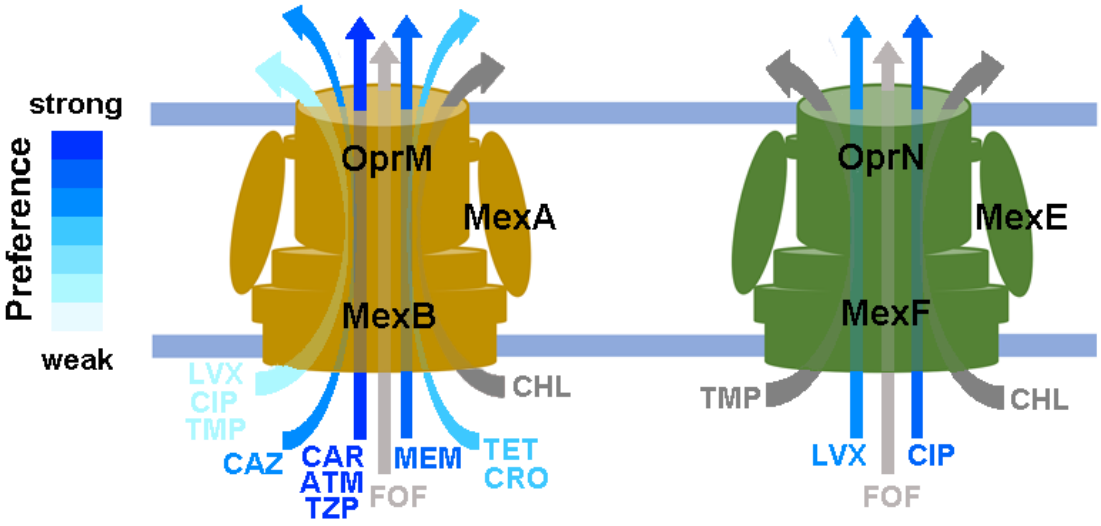

888

889

890 **Fig 6**

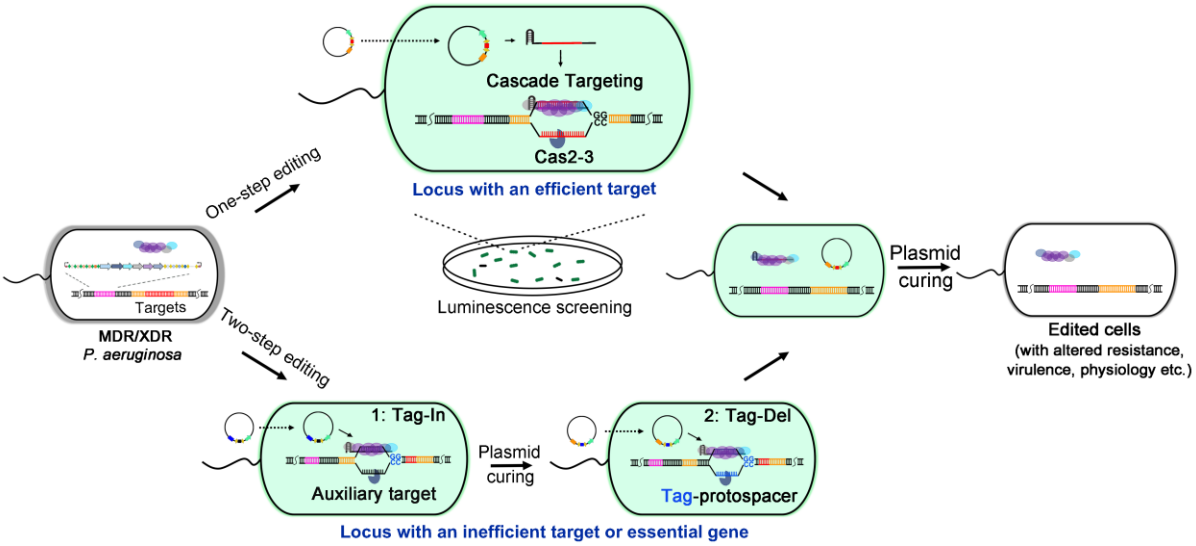

891